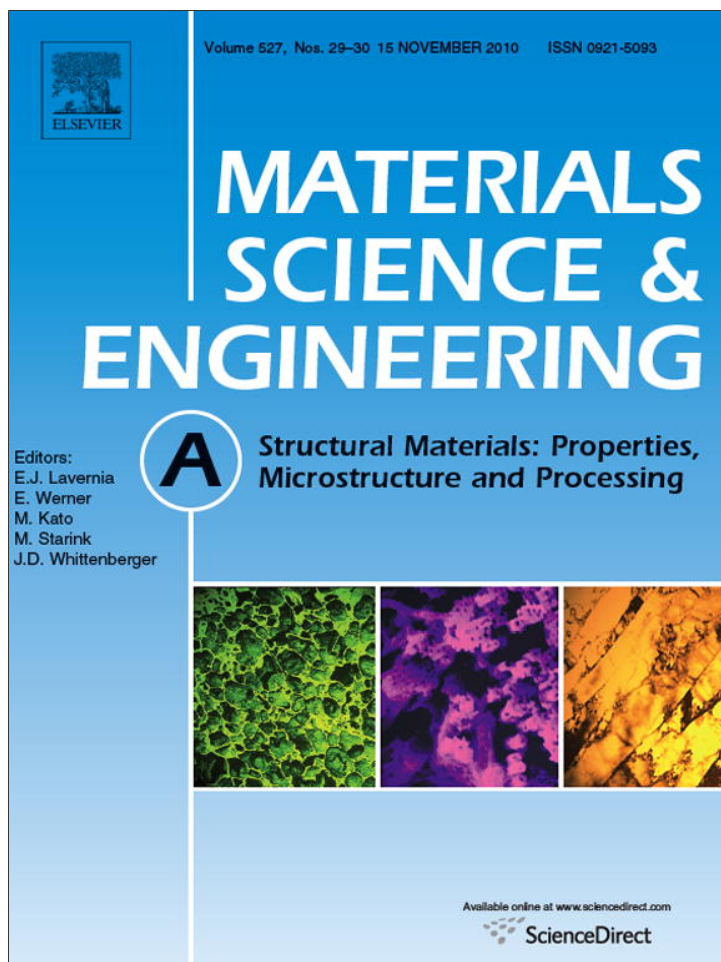


Provided for non-commercial research and education use.
Not for reproduction, distribution or commercial use.



This article appeared in a journal published by Elsevier. The attached copy is furnished to the author for internal non-commercial research and education use, including for instruction at the authors institution and sharing with colleagues.

Other uses, including reproduction and distribution, or selling or licensing copies, or posting to personal, institutional or third party websites are prohibited.

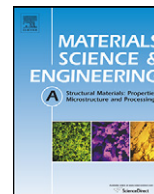
In most cases authors are permitted to post their version of the article (e.g. in Word or Tex form) to their personal website or institutional repository. Authors requiring further information regarding Elsevier's archiving and manuscript policies are encouraged to visit:

<http://www.elsevier.com/copyright>



Contents lists available at ScienceDirect

Materials Science and Engineering A

journal homepage: www.elsevier.com/locate/msea

Effect of die parameters and material properties in ECAP with parallel channels

F. Džavanroodi*, M. Ebrahimi

Department of Mechanical Engineering, Iran University of Science and Technology, Narmak, Tehran, Iran

ARTICLE INFO

Article history:

Received 26 May 2010

Received in revised form 31 July 2010

Accepted 9 August 2010

Keywords:

ECAP-PC

FEM

Die channel angle and displacement

Strength coefficient

Strain hardening exponent

ABSTRACT

In this paper, the influences of die parameters (die channel angle and channel displacement) and material properties (strength coefficient and strain hardening exponent) are investigated in equal channel angular pressing with parallel channels (ECAP-PC) using three dimensional (3D) finite element simulation (FEM). It has been shown that die parameters play an important role in the magnitude and homogeneity of effective strain. In general, die channel angle has more influence on the magnitude rather than homogeneity of effective strain, decreasing the die channel angle results in a higher magnitude of effective strain imposed on the sample and a higher pressing force. But on the other hand, channel displacement has more influence on the homogeneity of effective strain, increasing the die channel's displacement results in a more homogenous effective strain on the sample cross-section. Simulation on various strength coefficient and strain hardening exponents showed that the magnitude of the strain hardening exponent does not have much effect on the pressing force. On the other hand, the level of pressing force increases when the magnitude of the strength coefficient is increased.

© 2010 Elsevier B.V. All rights reserved.

1. Introduction

Equal channel angular pressing, developed by Segal [1], is one of the most prominent procedures among the various severe plastic deformation (SPD) techniques [2,3]. During ECAP, a sample is pressed through two intersecting channels with the same cross-sections and material is subjected to an intense plastic strain through simple shear [4]. The schematic diagram of ECAP die is shown in Fig. 1. The angle between the channels is defined by Φ and the outer corner angle is determined by Ψ . In ECAP, there are four fundamental routes that are shown in Fig. 2. Each route has a different slip system and imposes different strain value to the sample [5]. In route A, there is not any rotation. In route C, the sample rotates 180° after each pass. In routes B_A and B_C , a 90° rotation in an alternate direction and in the same direction are applied to the sample between consecutive passes [6]. By repeating the pressing process, a very high magnitude of strain is produced in the sample. This operation is time consuming, difficult to control and liable to operator error. To solve these problems, ECAP dies are created such as rotary-die, multi-pass-die and ECAP with parallel channels [7,8]. ECAP with parallel channels is shown in Fig. 3. Pressing the sample in this die is equivalent to pressing material in the classical ECAPed die after two passes with route C. The high magnitude of strain obtained in one pass is one of the important advantages of this die. In route C, the shearings take place on the same plane in

each consecutive pass, but the direction of the shear is reversed on the each pass. The sample receives a uniform effective strain distribution in comparison with other routes [9]. The magnitude of shear (γ) in the deformed sample is determined by assuming frictionless conditions [10]:

$$\gamma = 2 \cot\left(\frac{(\Phi + \Psi)}{2}\right) + \Psi \operatorname{cosec}\left(\frac{(\Phi + \Psi)}{2}\right) \quad (1)$$

Also, the magnitude of effective strain (ε) after N passes is given by the following relationship:

$$\varepsilon_{\text{eq}} = \frac{N}{3^{1/2}} \left[2 \cot\left(\frac{(\Phi + \Psi)}{2}\right) + \Psi \operatorname{cosec}\left(\frac{(\Phi + \Psi)}{2}\right) \right] \quad (2)$$

Eq. (2) represents the effective strain imposed to the sample during the ECAP process but does not show the local deformation behavior or in-homogeneity of strain distribution in the cross-section of the sample that is observed in experimental work. Finite element methods (FEM) have been widely used for the purpose of investigating the global and local deformation behavior with various die parameters. A number of FEM based analyses for classical ECAP die, especially for one pressing pass, have been reported in literature. Nagasekhar et al. investigated the effect of the die channel angle on the deformation behavior and punch pressure needed for extrusion [11]. Oruganti et al. explored the influence of backpressure, friction and strain rate sensitivity on the ECAP process [12]. Xu et al. studied distribution of strain in different die geometry and routes [13]. Kim et al. reported the effects of round corner in the strain behavior [14]. A modified ECAP die is investigated by Liang on the homogeneity of strain distribution [15]. Karpuz et al. surveyed the

* Corresponding author. Tel.: +98 21 77240203; fax: +98 21 77240203.
E-mail address: javanroodi@iust.ac.ir (F. Džavanroodi).

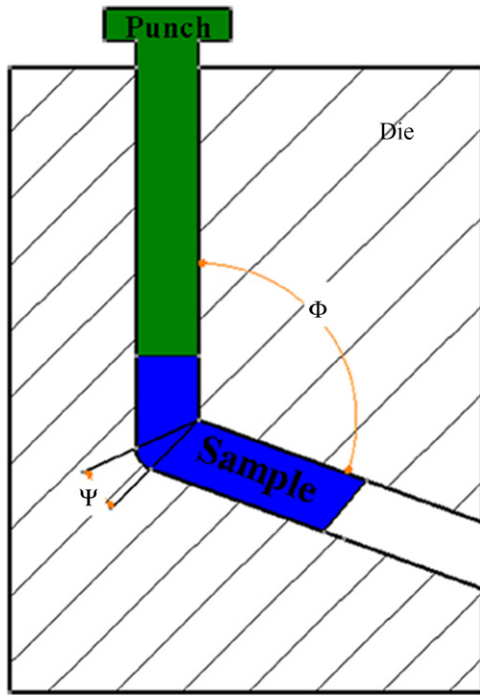


Fig. 1. Schematic diagram of the ECAP process.

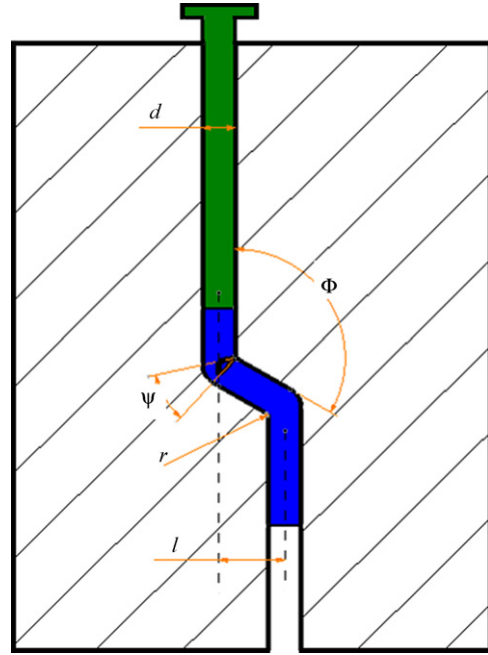


Fig. 3. Schematic diagram of the ECAP with parallel channels.

connection between material properties and dead zone angle [16]. Also, Prasanna Kumar et al. reported the influence of the die channel angle on the material flow by 3D FEM [17]. Djavaanroodi et al. [18] studied the influences of die channel angle, friction coefficient and back pressure in the ECAP die. They have reported that higher effective strain values can be obtained by using an acute die channel angle, high friction coefficient and applying back pressure. Also, there are number of experimental and analytical studies on ECAP with parallel channels [7,19–22]. Nakashima et al. [7] compared a multi-pass facility die which gave a total strain of approximately 5 on a single passage through the die with a die containing a single shearing plane. Experiments on purity aluminum showed that, at the same total strain both the hardness and the evolution of the microstructure are identical. Raab [19] used 2D FEM simulations to design and manufacture ECAP die with parallel channel. He showed that increasing die channel angle from 100° to 120° and die channel displacement from 0.5d to 1.5d, resulted in the enhancement of strain homogeneity in the cross-section. Liu et al. [20] showed that during ECAP with parallel channels, the originally equiaxed grains are elongated after passing the first bend and then returned to their original shape at the end of the pressing. TEM reports reveal that

formation of slip bands and twinning are the two important deformation mechanisms in Cu–Zn alloy. Studies by Zuyan and Zhongjin [21] exhibit that high pressing force are required by increasing the die channel angle value, the magnitude of friction coefficient, the length of sample and decreasing the gap between die and sample. Also, the effect of friction force is much larger than deformation force. It is seemed that more investigations are needed to scrutiny the influences of the die parameters and material properties on strain behavior and pressing force in ECAP-PC process. In this paper, the effect of the die channel angle (Φ), the distance between the two parallel channels (l) and material properties (strain hardened exponent (n) and strength coefficient (K)) are investigated by 3D FEM on an ECAP die with parallel channels. Also, the effective strain magnitude and in-homogeneity of strain on the cross-section of the sample has been studied. The pressing force required for extruding the sample is also calculated. To validate the numerical results, an ECAP die was designed and manufactured with the channel angle of 90° and the outer corner angle of 25°. Commercial pure aluminums were ECAPed one pass and the obtained data were used for validating the FEM model.

2. Finite element methods

For this study, finite element simulations were carried out using Deform-3D™ V5.0 with the plastic deformation behavior of the materials, as:

$$\bar{\sigma} = K\bar{\epsilon}^n \quad (3)$$

where $\bar{\sigma}$ is the effective von-mises stress, $\bar{\epsilon}$ is the effective plastic strain, K is the strength coefficient and n is the strain hardening exponent. The die and punch were assumed to be rigid, so that there is no deformation. The samples have the diameter of 8 mm and length of 60 mm with 3500 initial elements. The constant punch speed was 1 mm s⁻¹. Automatic re-meshing was applied to accommodate large deformation during the analysis and the symmetrical boundary conditions were applied because the model is symmetrical in the middle plane of the ECAP die. Friction coefficient of 0.1 is used for all simulations.

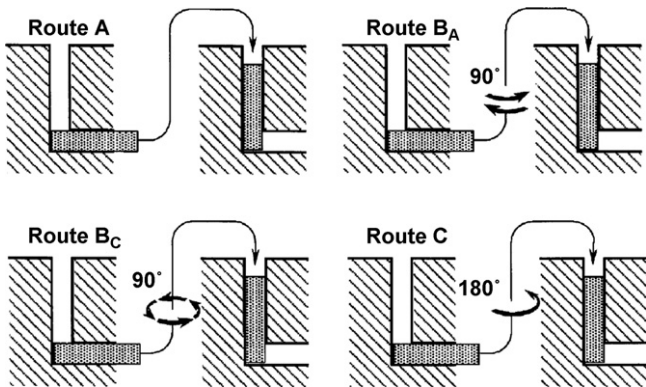


Fig. 2. Four fundamental routes in ECAP process.

Table 1

The chemical composition of commercial pure aluminum.

Material component	Aluminum, Al	Iron, Fe	Silicon, Si	Copper, Cu	Zirconium, Zr	Titanium, Ti	Magnesium, Mg
Percent	Base	0.212	0.100	0.015	0.013	0.009	0.007

In the first part of this paper, the die channel angles of 75°, 90°, 105° and 120° were simulated with the channels displacement of d , $1.5d$ and $2d$ where d is the diameter of the sample. The purpose of this part is to study the influence of die parameters on the magnitude of effective strain, in-homogeneity of strain at the cross-section of the sample and pressing force needed for extrusion. In the second part of this paper, the effects of material properties (K and n) on strain distribution are investigated. The influence of the strength coefficient and strain hardening exponent on the pressing force requirement are also studied. The magnitudes of the strength coefficient and strain hardening exponent that were used are: $K = 50$ MPa, 150 MPa, 250 MPa, 350 MPa and $n = 0.12, 0.16, 0.2, 0.24$. In all analysis (19 simulations), the outer corner angle is assumed equal to 20° and $r = 1$ mm.

3. Results and discussion

3.1. Validation of simulation analysis

To validate simulation results, ECAP die with the die channel angle of 90° and outer corner of 20° was used. Commercial pure aluminum was used that was homogenized at 670 °C for 0.5 h. The

chemical composition of pure Al is represented in Table 1. The speed of the punch was 1 mm s^{-1} and MoS_2 was used as lubrication. The diameter of the sample was 20 mm with a length of 100 mm. The magnitude of the strength coefficient ($C = 52$ MPa) strain hardening exponent ($n = 0.14$) was obtained using tensile testing according to ASTM B557M, 2006. The magnitude of the friction coefficient in the simulation condition was assumed as 0.1. The hydraulic press and ECAP die set-up are shown in Fig. 4. The deformed sample in experimental work and simulation analysis after one pass is shown in Fig. 5.

The punch force is a very important parameter in the experiment in order to verify the simulated results and to decide the optimum parameters such as the friction coefficient. Many factors will affect the result of the experiment; the accuracy of the sensors, the friction, the punch speed, the material property and so on will affect the final results. Moreover, the applied material properties and the simplification of the physical model will affect the simulated results. If the punch force in the simulation meets well with that in the experiment at the same punch position, the parameters used in the simulation are considered as the optimum. After one pass, the pressing pressure magnitudes obtained by the experimental work and the simulation results are 57 MPa and 54 MPa



Fig. 4. The ECAP set-up for experimental work: hydraulic press and ECAP die set-up.

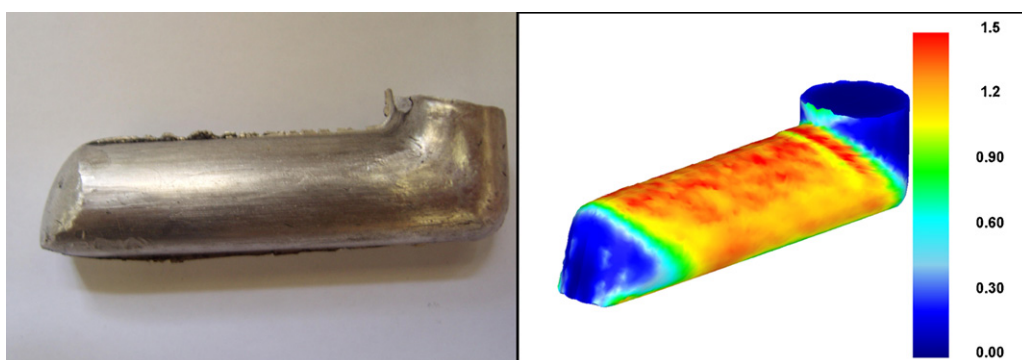


Fig. 5. The experimental and simulated ECAPed samples after one pass.

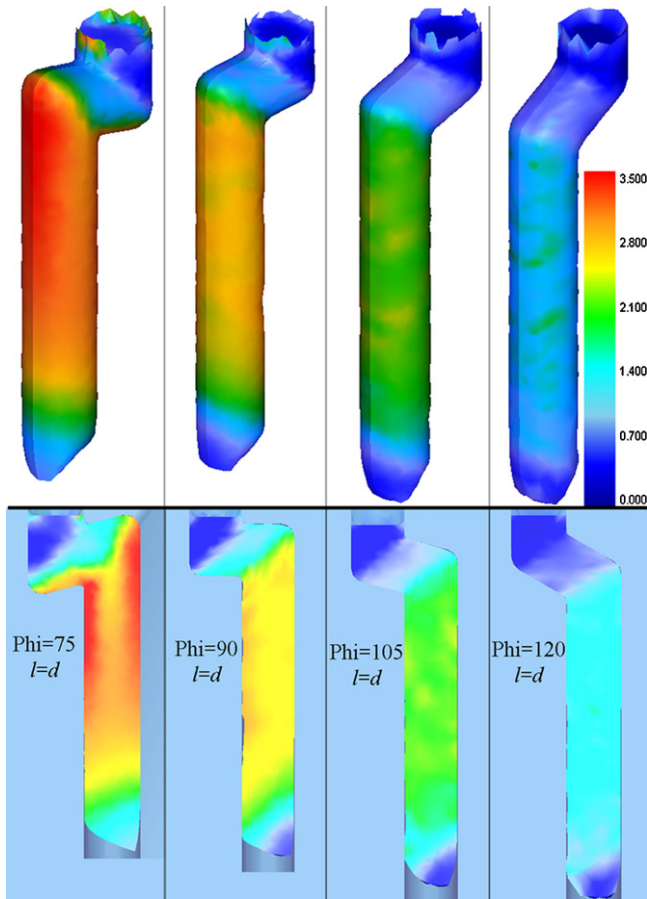


Fig. 6. 3D shapes and effective strain contours in the samples after the ECAP process for different die channel angles of 75°, 90°, 105°, 120° with the channel displacement of d .

respectively. This represents a 4% discrepancy between the experimental and the numerical results, which for all practical purposes is acceptable. Also, the magnitude of the effective strain achieved from simulation results and Eq. (1) are 1.09 and 1.05 respectively. Good agreement between experimental and simulation has been achieved.

The simulation running time for the sample with this geometry ($d = 20$ mm and $l = 100$ mm) was about 13 h. In order to reduce the computational running time the dimension of the sample was reduced to ($d = 8$ mm) for all of the analyses. With this new dimension the running time for each simulation was about 3 h.

3.2. Effect of die parameters

In order to obtain proper information about the deformation behavior of the sample during ECAP process, effective strain contours for $\Phi = 75^\circ, 90^\circ, 105^\circ, 120^\circ$ with $l = d, l = 1.5d$ and $l = 2d$ are shown in Figs. 6–8 respectively. It has been shown from previous studies that dead zone formation is a major factor for non-uniform strain distribution in classical ECAP dies [16]. During ECAP in the first bend, there is an under-filling of the outer corner of the die due to the formation of the dead zone, especially in the vicinity of the lower part of the deformed sample. When the sample reaches the second bend of the die, this part acts like back pressure for the first bend, which in turn prevents formation of the dead zone by filling up the outer corner region [18]. After that, the gap in the second bent begins to fill gradually and there is hardly any dead zone formation in this section. This back pressure will increase the homogeneity of the strain distribution in the vicinity of the lower

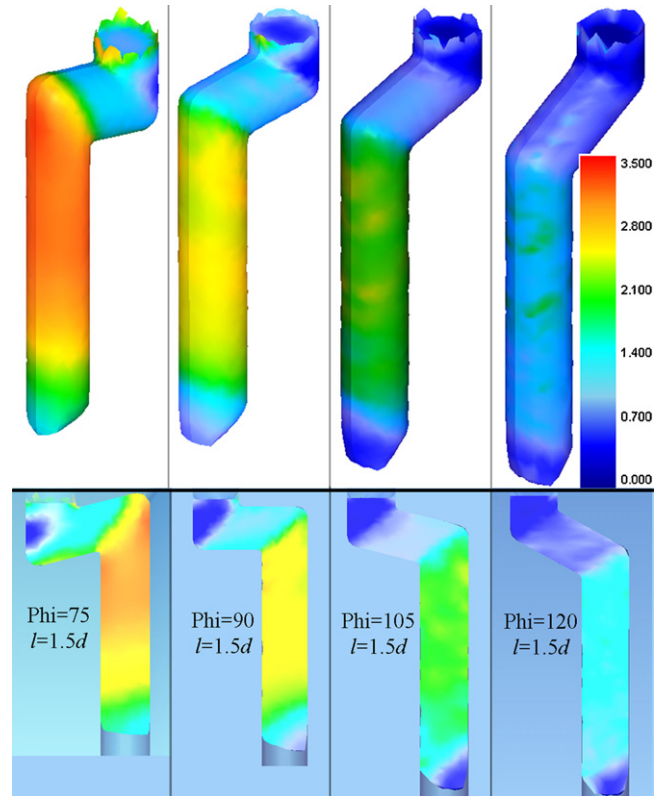


Fig. 7. 3D shapes and effective strain contours in the samples after the ECAP process for different die channel angles of 75°, 90°, 105°, 120° with the channel displacement of $1.5d$.

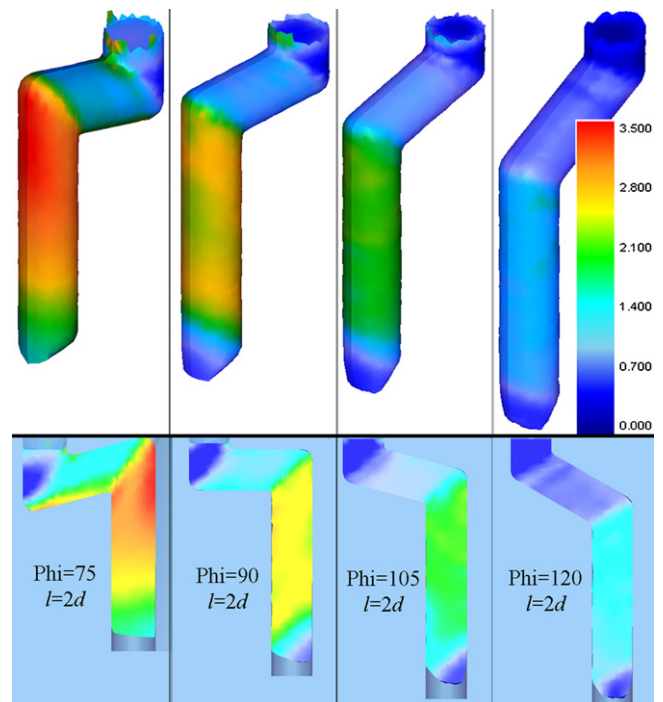


Fig. 8. 3D shapes and effective strain contours in the samples after the ECAP process for different die channel angles of 75°, 90°, 105°, 120° with the channel displacement of $2d$.

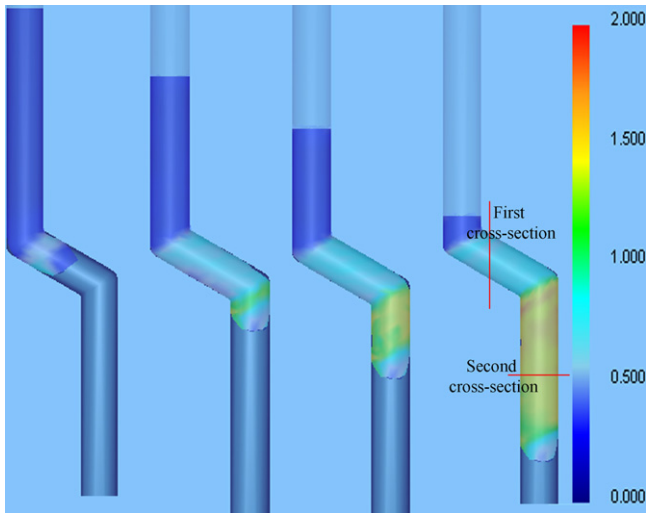


Fig. 9. Flow patterns of sample for the die channel angle of 120° with the channel displacement of 2d.

surface of the sample. This result has a good agreement with Rosochowski and Olejnik [23] and Wei et al. [24] findings. Hence, one of the advantages of this ECAP die is that there is hardly any formation of dead zone. This matter is shown in Fig. 9 for $\Phi = 120^\circ$ and $l = 2d$. It can be anticipated that the microstructure and properties of the material produced by ECAP with parallel channels is relatively isotropic.

The variation of die channel angles of $\Phi = 75^\circ, 90^\circ, 105^\circ, 120^\circ$ with channel displacements of $l = d, 1.5d, 2d$ can be seen more clearly in Fig. 10, where effective strain is plotted as a function of the die channel angle for different channel displacements. As can be observed, effective strain magnitude increases with decreasing the value of the die channel angle and reduction in the length of the channel displacement. With an increase in the die channel angle to 120° from 75°, the magnitude of the effective strain is decreased to 1.27 from 2.36 with the channel displacement of d . Also, the effective strain value reduces to 2.16 from 2.36, when the channel displacement is increased to $2d$ from d with the die channel angle of 75°. So the lowest magnitude of the effective strain is related to $\Phi = 120^\circ, l = 2d$ and the highest magnitude of the effective strain is associated to $\Phi = 75^\circ, l = d$. The result for the die channel angle of 120° by the channel displacement of $l = 2d$ has a good agreement with Suo's studies for the friction coefficient of 0.1 [25].

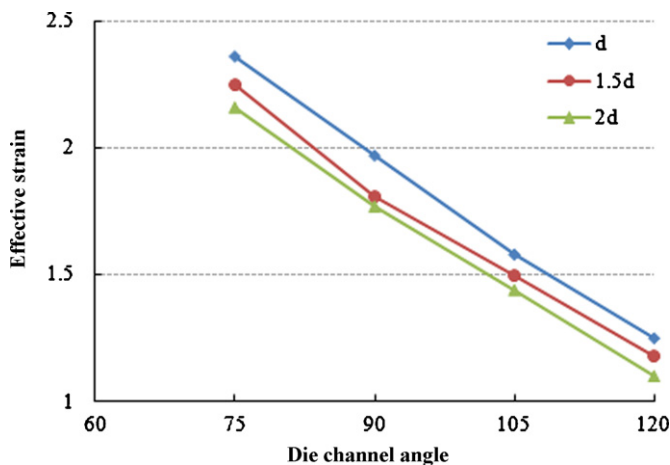


Fig. 10. Magnitudes of effective strain obtained for $\Phi = 75^\circ, 90^\circ, 105^\circ, 120^\circ$ and $l = d, 1.5d, 2d$.

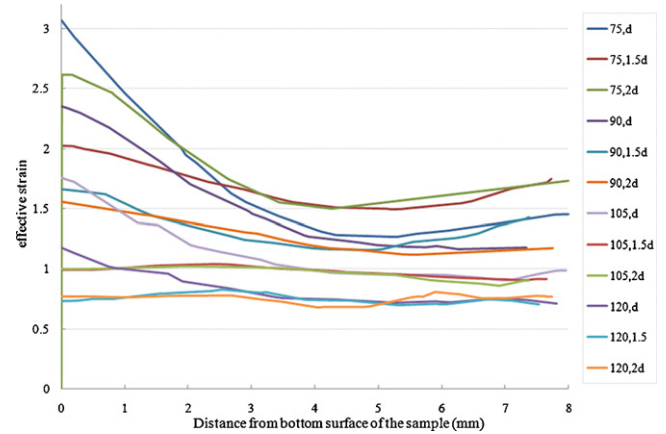


Fig. 11. Effective strain distribution in the first cross-section of the sample with various die channel angles of $\Phi = 75^\circ, 90^\circ, 105^\circ, 120^\circ$ and different channel displacements of $l = d, 1.5d, 2d$.

For better understanding of the non-uniform distribution of strain, Figs. 11 and 12 show the distribution of effective strain in the first and second cross-sections of the sample. The coordinates of the first and second cross-sections are shown in Fig. 9. For these cross-sections, for channel displacements of $l \geq 1.5d$ more uniformity of effective strain has been achieved irrespective of the die channel angle. In-homogeneity index is used to investigate details of Fig. 12. The degree of in-homogeneity is defined as [17]:

$$C_i = \frac{\varepsilon_{max} - \varepsilon_{min}}{\varepsilon_{ave}} \quad (4)$$

where ε_{max} , ε_{min} and ε_{ave} are maximum, minimum and average values of strain value in the second cross-section of the sample respectively. More homogeneity of strain distribution is obtained by reducing the magnitude of C_i and closing it to zero. The magnitudes of in-homogeneity index (C_i) for various die channel angles and channel displacements in the second cross-section are given in Table 3. As can be observed, as the number of passes increases for all channel angle and channel displacement the homogeneity of strain increases. Also, increasing channel displacement causes more homogeneity of strain distribution in the cross-section of the sample. In general, decreasing die channel angle and channel displacement cause a higher magnitude of effective strain in the whole sample. Although both of these parameters have affect on the effec-

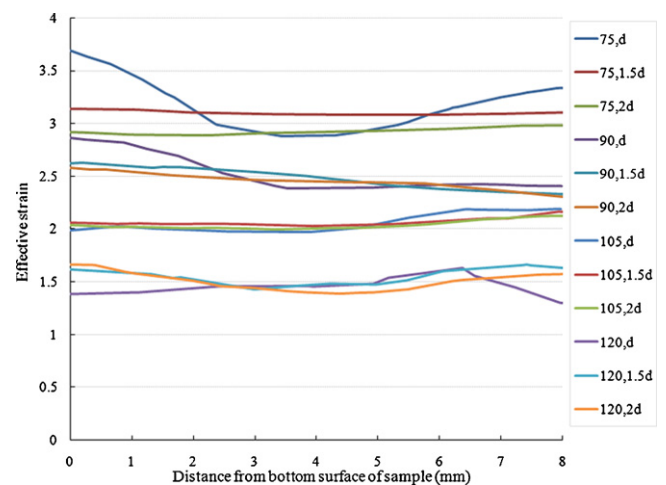


Fig. 12. Effective strain distribution in the second cross-section of the sample with various die channel angles of $\Phi = 75^\circ, 90^\circ, 105^\circ, 120^\circ$ and different channel displacements of $l = d, 1.5d, 2d$.

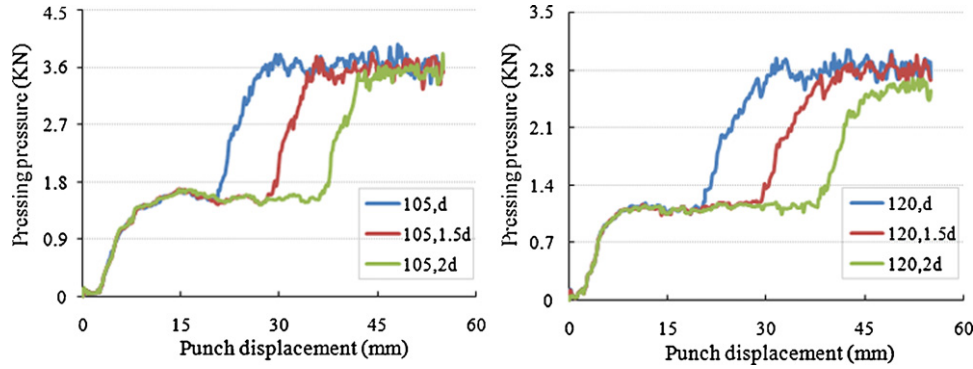


Fig. 13. Diagrams of pressing force versus punch displacement for the two die channel angles of 105° and 120° with three channel displacements of $l = d, 1.5d, 2d$.

Table 2
The magnitudes of effective strain and pressing force for ECAP ($\psi^\circ = 25^\circ, r = 1 \text{ mm}, m = 0.1$).

	Φ°	$l (d = 8 \text{ mm})$	ϵ_{total}	$F(\text{KN})$ (first bent)	$F(\text{KN})$ (total)
Die 1	75	d	2.36	3.20	5.10
Die 2	75	$1.5d$	2.25	3.25	5.40
Die 3	75	$2d$	2.16	3.20	5.50
Die 4	90	d	1.97	2.30	4.60
Die 5	90	$1.5d$	1.81	2.35	4.40
Die 6	90	$2d$	1.77	2.40	4.45
Die 7	105	d	1.58	1.65	3.85
Die 8	105	$1.5d$	1.50	1.60	3.85
Die 9	105	$2d$	1.44	1.60	3.70
Die 10	120	d	1.25	1.15	3.05
Die 11	120	$1.5d$	1.18	1.15	3.00
Die 12	120	$2d$	1.10	1.16	2.85

tive strain magnitude and homogeneity of strain distribution, but the most effect of die channel angle is on the effective strain magnitude and the highest influence of channel displacement is on the homogeneity of strain distribution. On the other words, die channel angle for controlling effective strain magnitude and channel displacement for controlling homogeneity of strain distribution are suitable.

The pressing force versus punch displacement curves are shown in Fig. 13 for the two die channel angles of 105° and 120° with three channel displacements of $d, 1.5d$ and $2d$. Referring to this figure, the pressing force increases with the punch movement until it reaches a stable level. This magnitude of force is needed for extruding the sample through the first bend; higher force is required for continuing the process, so that sample passes through the second bend. By increasing the magnitude of the channel displacement (l), the second pressing force is delayed because of the long distance which exists between the two parallel channels. So, the applicability of this ECAP die is limited by the die set working capacity especially for acute die channel angles. As a snapshot and summary for this part of the research, Table 2 is represented at different die conditions. It is interesting to note that an increase in the channel displacement causes higher pressing force for $\Phi < 90^\circ$; but lower pressing force is required with increasing channel displacement for $\Phi \geq 90^\circ$. In general, a higher magnitude of pressing force is required as the die channel angle value increases [20].

Table 3
The magnitudes of in-homogeneity index for various die channel angles and channel displacements at first and second cross-sections.

Φ°	d				$1.5d$				$2d$			
	75	90	105	120	75	90	105	120	75	90	105	120
C_i at first cs	1.07	0.79	0.77	0.56	0.32	0.38	0.14	0.17	0.62	0.34	0.17	0.19
C_i at second cs	0.26	0.20	0.12	0.23	0.02	0.13	0.09	0.15	0.03	0.13	0.07	0.18

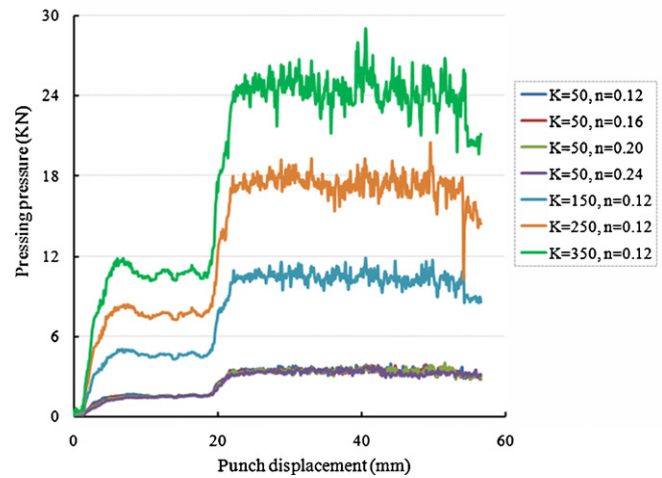


Fig. 14. Diagrams of pressing force versus punch displacement for different material properties.

3.3. Effect of material properties

Various magnitudes of strength coefficient and strain hardening exponents have been investigated on the pressing force and strain behavior. First, the strength coefficient magnitude was kept constant at 50 MPa and four strain hardening exponents of 0.12, 0.16, 0.2 and 0.24 were analyzed. Finally, four strength coefficients of 50 MPa, 150 MPa, 250 MPa and 350 MPa with a strain hardening exponent of 0.12 were simulated. The purpose of these analyses is to investigate the effect of material properties on the magnitude of the pressing force for deforming the sample. Fig. 14 shows the curves of pressing force needed to extrude sample with different strength coefficients and strain hardening exponents. As can be seen, the magnitude of the strain hardening exponent does not have much effect on the pressing force. The same values in the pressing force are obtained by different magnitudes of the strain hardening exponent; but for various magnitudes of the strength coefficient, different values of pressing forces are achieved. A higher pressing force is required with an increase in the magnitude of the strength coefficient. The pressing force in the first bend (before the sample reaching the second bend) decreases 88% when the magnitude

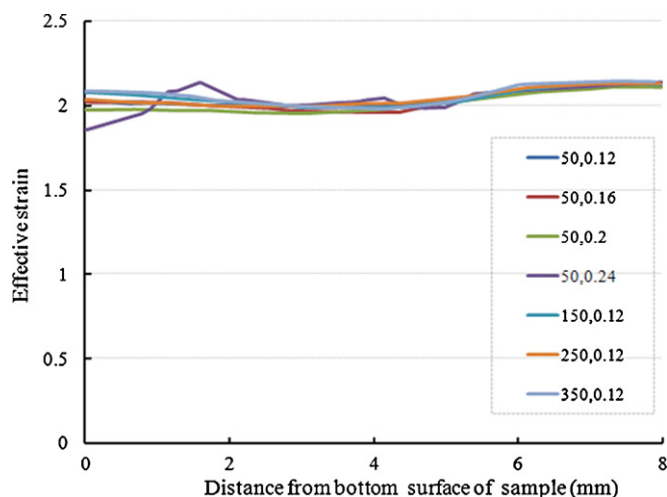


Fig. 15. Diagrams of pressing force versus punch displacement for four strength coefficients of 50 MPa, 150 MPa, 250 MPa and 350 MPa with four strain hardening exponents of 0.12, 0.16, 0.2 and 0.24.

of the strength coefficient decreases to 50 MPa from 350 MPa with the same strain hardening exponent ($n = 0.12$). Also an 87% reduction is obtained in the pressing force after the second bend with above material property conditions. By contrasting the simulation results, the same magnitude of effective strain is obtained, so it can be assumed that material properties do not have any effect on the strain behavior. The same distribution of effective strain is achieved in ECAPed samples with different material properties. Fig. 15 shows the effective strain behavior in the second cross-section (after the second bent) for various material properties.

4. Conclusion

The behavior of die parameters and material properties in ECAP was investigated by using 3DFEM and an experimental method. From this study, the following conclusions were drawn:

1. In ECAP with parallel channels process, the die channel angle and channel displacement play an important role in the magnitude of effective strain. Decreasing the die channel angle and channel displacement cause a higher magnitude of effective strain that is imposed to the sample. In general, die channel angle has more influence on the magnitude rather than homogeneity of effective strain, decreasing the die channel angle results in a higher magnitude of effective strain imposed on the sample and a higher pressing force. But on the other hand, channel displacement has more influence on the homogeneity of effective strain, increasing the die channel's displacement results in a more homogenous effective strain on the sample cross-section.
2. Various strength coefficients and strain hardening exponents were simulated to estimate the value of the pressing force. The

different magnitudes of strain hardening exponents do not have much effect on the pressing force value; but an increase in the magnitude of the strength coefficient causes a higher magnitude of pressing force.

3. Elimination of dead zone and more homogeneity of effective strain distribution in the ECAPed sample's cross-section are the advantages of this ECAP die.

To validate simulation results, theoretical and experimental values were compared with simulation results and there was a good agreement between them.

References

- [1] V.M. Segal, *Materials Science and Engineering A* 271 (1999) 322–333, PII: S0921-5093(99)00248-8.
- [2] C. Xu, M. Furukawa, Z. Horita, T.G. Langdon, *Journal of Alloys and Compounds* 378 (2004) 27–34, doi:10.1016/j.jallcom.2003.10.065.
- [3] M. Furukawa, Z. Horita, M. Nemoto, T.G. Langdon, *Materials Science and Engineering A* 324 (2002) 82–89, PII: S0921-5093(01)01288-6.
- [4] M. Furukawa, Y. Iwahashi, Z. Horita, M. Nemoto, T.G. Langdon, *Materials Science and Engineering A* 257 (1998) 328–332, PII: S0921-5093(98)00750-3.
- [5] V.V. Stolyarov, Y. Theodore Zhu, I.V. Alexandrov, T.C. Lowe, R.Z. Valiev, *Materials Science and Engineering A* 299 (2001) 59–67, PII: S0921-5093(00)01411-8.
- [6] T.G. Langdon, *Materials Science and Engineering A* (2006), doi:10.1016/j.msea.2006.02.473.
- [7] K. Nakashima, Z. Horita, M. Nemoto, T.G. Langdon, *Materials Science and Engineering A* 281 (2000) 82–87, PII: S0921-5093(99)00744-3.
- [8] J.-C. Kim, Y. Nishida, H. Arima, T. Ando, *Materials Letters* 57 (2003) 1689–1695, PII: S0167-577X(02)01053-4.
- [9] S. Xu, G. Zhao, Y. Luan, Y. Guan, *Journal of Materials Processing Technology* 176 (2006) 251–259, doi:10.1016/j.jmatprotec.2006.03.167.
- [10] W.J. Kim, J.C. Namkung, *Materials Science and Engineering A* 412 (2005) 287–297, doi:10.1016/j.msea.2005.08.222.
- [11] A.V. Nagasekhar, T.-H. Yip, S. Li, H.P. Seow, *Materials Science and Engineering A* 410–411 (2005) 269–272, doi:10.1016/j.msea.2005.08.043.
- [12] R.K. Oruganti, P.R. Subramanian, J.S. Marte, M.F. Gigliotti, S. Amancherla, *Materials Science and Engineering A* 406 (2005) 102–109, doi:10.1016/j.msea.2005.06.031.
- [13] S. Xu, G. Zhao, X. Ma, G. Ren, *Journal of Materials Processing Technology*, doi:10.1016/j.jmatprotec.2006.11.025.
- [14] H.S. Kim, M.H. Seo, S.I. Hong, *Journal of Materials Processing Technology* 130–131 (2002) 497–503, PII: S0924-0136(02)00796-3.
- [15] S. Wang, W. Liang, Y. Wang, L. Bian, K. Chen, *Journal of Materials Processing Technology* 209 (2009) 3182–3186, doi:10.1016/j.jmatprotec.2008.07.022.
- [16] P. Karpuz, C. Simsir, C. Hakan Gür, *Materials Science and Engineering A* 503 (2009) 148–151, doi:10.1016/j.msea.2008.01.095.
- [17] V. Patil Basavaraj, U. Chakkingal, T.S. Prasanna Kumar, *Journal of Materials Processing Technology* 209 (2009) 89–95, doi:10.1016/j.jmatprotec.2008.01.031.
- [18] F. Djavanroodi, M. Ebrahimi, *Materials Science and Engineering A* 527 (2010) 1230–1235, doi:10.1016/j.msea.2009.09.052.
- [19] G.I. Raab, *Materials Science and Engineering A* 410–411 (2005) 230–233, doi:10.1016/j.msea.2005.08.089.
- [20] Z.Y. Liu, G.X. Liang, E.D. Wang, Z.R. Wang, *Materials Science and Engineering A* 242 (1998) 137–140, PII: S0921-5093(97)00467-X.
- [21] L. Zuyan, W. Zhongjin, *Journal of Materials Processing Technology* 94 (1999) 193–196, PII: S 0924-0136(99)00096-5.
- [22] R.Z. Valiev, T.G. Langdon, *Progress in Materials Science* 51 (2006) 881–981.
- [23] A. Rosochowski, L. Olejnik, *Journal of Materials Processing Technology* 125–126 (2002) 309–316, PII: S0924 0136(02)00339-4.
- [24] W. Wei, A.V. Nagasekhar, G. Chen, T.-H. Yip, K.X. Wei, *Scripta Materialia* 54 (2006) 1865–1869, doi:10.1016/j.scriptamat.2006.02.026.
- [25] T. Suo, Y. Li, Q. Deng, Y. Liu, *Materials Science and Engineering A* 466 (2007) 166–171, doi:10.1016/j.msea.2007.02.068.